An Electrostatic Probe for Laser Beam Welding Diagnostics

A simplified theory for determining electron density is validated by probes into the laser plume

BY A. J. RUSSO, R. L. AKAU AND D. M. KEICHER

ABSTRACT. In laser beam welding it has been found that the interaction of the material vaporized from the surface with the incoming laser beam can strongly affect the size and shape of the weld produced. To understand the physics of this interaction, measurements of the characteristics of the vapor plume produced are desirable. Diagnostic measurements of temperature, pressure and electron density on pulsed laser weld vapor plumes are difficult because of the short times and high temperatures involved. The use of electrostatic probes to make such measurements has been investigated and is the subject of this paper. A simplified electrostatic probe theory has been developed and applied to the data taken from probe measurements on aluminum and steel samples welded by a Nd:YAG pulsed laser.

Introduction

An experimental means of determining the electron density of the plasma in the vapor plume produced by a laser beam weld would be useful as a diagnostic tool for determining temperature, pressure, or possible nonequilibrium effects of electrical breakdown of the plume by the high-density incident beam. Since the zone above the weld is small (typically less than 1 mm in diameter) and the vapor plume is only present for a few milliseconds in pulsed welding, this is not an easy measurement to make. Spectroscopic measurements of temperature in this region have been made by H. C. Peebles at Sandia National Labs for Nd:YAG pulsed welds on aluminum (Ref. 1). These measurements indicate that the vapor plume is close to the boiling temperature for incident power densities of $\approx$5000 W/mm^2. If thermochemical equilibrium is assumed, the electron density can be calculated with ordinary chemical equilibrium models.

In order to verify these measurements, it would be useful to obtain an independent measure of the electron density in this region. Electrostatic probes are one possible way to make such a measurement (Refs. 2, 3). Although the construction and use of such probes are relatively simple, the data interpretation to obtain the desired parameters is not. This paper will develop a simplified theory for the interpretation of data from a hollow cylindrical probe operating in the pressure and temperature range typical of laser vapor plumes, and apply it to the data taken from probe measurements of pulsed laser weld plumes.

Probe Geometry

An electric probe consists of two metallic electrodes in contact with the ionized gas that is to be measured. Figure 1 shows a sketch of the geometry of the cylindrical probe used. The workpiece itself serves as one of the electrodes, and a thin (0.25-mm/0.01-in.) strip of molybdenum with a hole in it just large enough (1 mm/0.04 in.) to pass the laser beam is the other electrode. All surfaces of the molybdenum strip, except that of the interior of the hole, are covered by an electrically insulating Kapton film 0.127 mm thick. The molybdenum strip is placed flat on the workpiece and aligned so that the laser beam passes through the hole. With this arrangement, the active probe surfaces are the molten weld pool directly under the hole and the interior hole surface. The advantages of this geometry are: contact with the gas of interest is obtained without obstructing the laser beam or destroying the probe; enclosure of the flowing plume adjacent to the surface inhibits entrainment of air in that region, which would cool the plume and change its properties; and a relatively simple computational region is produced so that the numerical solution of Laplace's equation required for data interpretation is made easy.

There are two ways that the electrodes can be connected. The first is with the workpiece as the anode and the probe strip as the cathode. With that connection, the current-voltage characteristic will exhibit a near-saturation effect as the voltage increases. Most of the applied voltage will be dropped across a very thin charged layer (the sheath) adjacent to the cathode. The saturation current can be interpreted as the natural ion diffusion rate at the edge of the sheath nearest the hot gas. Since this diffusion current is proportional to the ion number density and square root of temperature at the edge of the sheath, a very simple estimate of either of these properties can be made if the other is known. In addition, the slope of the current-voltage characteristic near the zero-current region can be related to the electron temperature (Ref. 2).

The disadvantage of this connection is that the properties measured are those of the gas at the edge of the hole. That gas is out of the laser beam and only at the edge of any possible plume-beam interaction. It also may be cooler than the core-flow gas because it is near a cool surface. The other possible connection reverses the polarity so that the workpiece is the cathode. The gas at the edge of the cathode sheath would then be the core-flow gas (generated by vaporization

KEY WORDS

Electrostatic Probe
Welding Diagnostics
Pulsed Laser Welding
Temperature Measures
Pressure Measures
Electron Density
Vapor Plume
Probe Measurements
Nd:YAG Pulsed Laser
Aluminum and Steel

A. J. RUSSO and R. L. AKAU are with the Fluid and Thermal Sciences Department, and D. M. KEICHER is with the Process Metallurgy Division, Sandia National Laboratories, Albuquerque, N. Mex.

at the cathode) and is directly in the laser path. The disadvantage of this connection is that the cathode is at the vaporization temperature and will be thermionically emitting electrons. The current-voltage characteristic may no longer exhibit saturation at voltages low enough that the plasma is not disturbed by energy input from the probe, and the easy interpretations of probe data made with the first connection are no longer possible. However, in the regimes of interest for many laser beam welding problems, a simplified theory for that case can be applied to low-voltage data. This theory is developed in the next section.

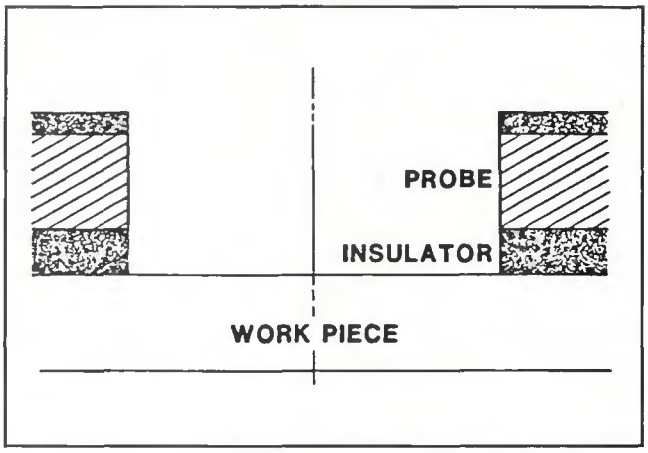

Fig. 1 — A sketch of the cylindrical electrostatic probe geometry

Theory

The usual approach to solving continuum probe problems is to write species conservation equations for ions and electrons, and Poisson's equation to relate the electric potential to the net charge density at a point and solve the system numerically (Ref. 4). The neutral density, temperature and velocity are taken from an uncoupled fluid dynamics solution. This approach works well for low-density plasmas (with electron densities less than 10^{12} cm^{-3}) but becomes more difficult as the number density increases because the equations become stiff and resolution of the sheath requires very fine gridding. A thermionic emission boundary condition at the cathode further complicates the present problem, which typically involves electron densities of 10^{14} cm^{-3}. For those reasons, a simpler approach will be taken.

The assumptions used in developing the probe equations to be used are:

1) The plume in the probe region (bounded by the work surface, the cylindrical hole wall and the outside surface of the strip) can be divided into three zones: a core-flow zone occupying most of the volume in which the plasma is homogeneous, isothermal, neutral, and moving straight up with a velocity U; an anode sheath zone which is negatively charged; and a cathode sheath zone which has both electron-rich and positive-ion-rich structure.

2) The vapor is singly ionized.

3) There is frozen chemistry in the sheath regions.

4) All the particles diffusing into a sheath region, in which there is no retarding potential, reach the electrode.

5) No air is entrained in the vapor plume until it exits the probe region, after which it cools rapidly and no currents are carried outside the probe region.

For most of the metal vapor plumes observed, the velocities have been less than tens of meters per s; therefore, the Reynolds number is low and the boundary layer can grow rapidly. The constant velocity assumption in the first consideration is weak, but it has little influence on the solutions because field-induced and diffusive velocities dominate these low-convective motions. Because most vapors have a high heat of vaporization, the effective Prandtl number near the vaporization temperature becomes very large and the thermal boundary layer becomes small so that the isothermal assumption is justified.

The voltage applied to the probe[1] V results in voltage drops across three regions: in the anode sheath, V_a; the core-flow plasma, V_p; and the cathode sheath, V_c.

Anode Region

For a voltage rise from anode to sheath edge less than the floating potential $V_{float} = \frac{kT}{e} \ln \sqrt{\frac{T_e m_i}{T_i m_e}}$ the current density at the anode, j_a, is related to voltage drop across the anode sheath by

$$j_a = -en\left(\frac{kT_i}{2\pi m_i}\right)^{1/2} + en\left(\frac{kT_e}{2\pi m_e}\right)^{1/2} \exp\left(\frac{eV_a}{kT_e}\right) \qquad (1)$$

where e is the absolute value of the electronic charge, n is the charged species number density, T is the temperature, m is the mass, and the subscripts i and e refer to ions and electrons, respectively.

The first term on the right represents the natural ion diffusion current to the anode and will be referred to as the ion saturation current density, j_{is}. The second term on the right represents the electron diffusion current to anode, which is reduced because of the retarding potential, V_a (which is negative).

Equation 1 may be solved for the potential of the plasma at the anode sheath edge with respect to the anode, $-V_a$

$$-V_a = \frac{kT_e}{e} \ln \sqrt{\frac{T_e m_i}{T_i m_e}} - \frac{kT_e}{e} \ln\left(\frac{j_a}{j_{is}} + 1\right) \qquad (2)$$

Core-Flow Region

For the core-flow plasma, it will be assumed that the electron and heavy particle temperatures are approximately equal. The conductivity of the plasma σ in this region is

$$\sigma = ne^2\left(\frac{1}{m_e \nu_e} + \frac{1}{m_i \nu_i}\right) \qquad (3)$$

where ν is the collision frequency. Using the relationship for diffusion coefficient of a charged species in a neutral gas $D = kT/m\nu$, and $\beta = D_i/D_e = \sqrt{m_e/m_i}$, the conductivity may be written in terms of the diffusion coefficient of the ions.

$$\sigma = \frac{ne^2 D_i}{kT}\left(\frac{1}{\beta} + 1\right) \qquad (4)$$

For a constant conductivity, the solution of the Laplace equation over the core-flow region will give the potential field distribution in the core. The gradient of that field times the conductivity will give the current density, and integration of the current density over the electrodes gives the probe current. In order to solve the Laplace equation, however, the potential boundary conditions over the core-flow region must be known. The potential at anode sheath edge can be obtained from Equation 2, and a similar equation must be obtained for cathode sheath edge.

Cathode Region

Before developing the cathode sheath current-voltage relation, some current

[1] *If the anode and cathode are different materials, the work function difference $W_c - W_a$ must be added to the external voltage to obtain the applied voltage.*

magnitude scoping calculations will be done so that some simplifying assumptions can be made. The natural ion diffusion current density at the cathode sheath is given by the same relation as the ion saturation current density at the anode sheath (see Equation 1). For an aluminum weld at atmospheric pressure, the vapor plume temperature is approximately 3000 K. The equilibrium ionization density, n, is 1.8×10^{20} m^{-3}. The mass of an aluminum ion is 4.5×10^{-26} kg. The ion saturation current density is then $j_{is} = 1.1 \times 10^4$ A/m^2. The electron saturation current density is $\sqrt{m_i/m_e} = 222$ times this value, so that $j_{es} = 2.45 \times 10^6$ A/m^2. Saturation electron emission current density can be calculated from the Richardson equation (Ref. 5) which is

$$j_{em} = AT^2 \exp \frac{-e\phi}{kT} \qquad (5)$$

where A is Richardson's constant and is ≈600,000 for most metals, and ϕ is the work function, which for aluminum is taken as 4.2 V (Ref. 6).

With these values, $j_{em} = 4.75 \times 10^5$ A/m^2. Since the electron emission current is more than an order of magnitude larger than the ion saturation current, but much less than the electron saturation current, there will still need to be a positive ion sheath to retard the incoming electrons. Close to the cathode, however, there are sufficient electrons emitted to totally neutralize any ions present and to form an electron sheath. This two-structure sheath for electron emitting probes has been treated in Ref. 7. Under these conditions, the electron current actually leaving the electron sheath area will be space charge limited. The electron mean free path in air at 3000 K is $\approx 5.6 \times 10^{-6}$ m (Ref. 8), and it is assumed that it is of the same order in aluminum vapor. The Debye length ($69\sqrt{T/n}$) is 2.8×10^{-7} m. Since mean free path is much larger than Debye length, the electron sheath may be considered collisionless and the space charge limited current density, j_{scl}, may be estimated by (Ref. 5)

$$j_{scl} = 2.33 \times 10^{-6} \frac{V_c^{3/2}}{d^2} \qquad (6)$$

where d is the total cathode sheath thickness and is approximately 30–50 Debye lengths (Ref. 4). Assuming d = 50 Debye lengths, $j_{scl} \approx 1.2 \times 10^4 V_c^{3/2}$ which is approximately equal to the ion saturation current density for sheath potentials on the order of 1 V.

The total cathode current density may then be written

$$j = j_{is} - j_{es} \exp\left(\frac{-eV_c}{eT_e}\right) + j_{scl} \qquad (7)$$

Substituting the appropriate expressions for the j's this may be written as

$$V_c = V_{float} - \frac{kT}{e} \ln\left(1 - \frac{j}{j_{is}} + \frac{j_{scl}}{j_{is}}\right) \qquad (8)$$

or

$$V_c = \frac{kT}{e}\left[\ln(222) - \ln\left(1 - \frac{j}{j_{is}} + \frac{j_{scl}}{j_{is}}\right)\right] \qquad (9)$$

For probe currents on the order of the ion saturation current, the second log term is smaller than the first and represents a perturbation around the floating potential. The cathode potential is not very sensitive to the estimate used for the sheath thickness d (a 67% change in d results in a 17% change in V_c), and a value of d = 50 Debye lengths was assumed for the calculated results shown in this paper.

Materials such as iron or nickel, which have higher ionization potentials, are found to have electron emission current densities approximately equal to the electron saturation current at one atmosphere and vaporization temperature. In those cases, the emission current will still be space charge limited and the same arguments given above are still applicable.

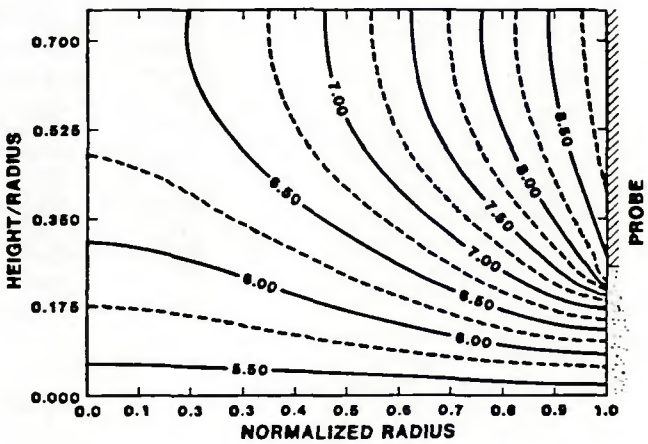

Fig. 2 — Calculated equipotential lines in the right half of the axisymmetric probe core-flow region

Expressions for the potential at the boundaries of the core-flow region next to the electrodes have now been given. The assumption that no current flow outside this region implies that $\frac{\partial V}{\partial z} = 0$ at the upper boundary and from symmetry $\frac{\partial V}{\partial r} = 0$ at the centerline, and all the boundary conditions necessary to solve the Laplace equation are available (although they must be iterated with the solution since the anode and cathode voltage conditions depend on the current density).

When the voltage applied to the probe is less than a few volts, the above equations may be iteratively solved for the probe current for various assumed values of temperature and pressure, and comparisons of data with these calculated current-voltage characteristics permit an estimate of temperature to be made.

Figure 2 shows a contour plot of the equipotential lines in the right-half zone of the axisymmetric computational region. This calculation corresponds to a 1-V applied potential to an isothermal aluminum vapor plasma at 3000 K. The current density distribution that this potential field produces is shown in Figs. 3 and 4 for the workpiece and probe, respectively. It is seen that most of the current flows from the lower portion of the probe to the outer half of the beam spot on the workpiece.

Field-Induced Electron Density

The derivations given above have been made under the assumption that the electron and ion temperatures were the same and that the presence of the applied probe potential did not change the electron number density. This will be true if the ratio of electric field strength to pressure is below 50 V/m-torr (Ref. 9). A correction for the enhancement of the electron number density due to the presence of the electric field may be made as follows.

The electric field strength in the core-flow region may be estimated by dividing the applied probe voltage by the average current flow path length (≈ the insulator thickness) or actually calculated locally from the Laplace equation or Equation 13. The average thermal velocity of the electrons c_e may be calculated from the solution to the Langevin equation (Ref. 8),

$$c_e = \left[\frac{2}{k}\left(\frac{eE}{m_e \nu_e}\right)^2 + \left(\frac{m_i}{m_e}\right)c_i^2\right]^{1/2} \qquad (10)$$

where k is the fraction of energy lost by collision by an electron, E is the electric field strength, ν_e is the electron collision frequency, and c_i is the thermal speed of

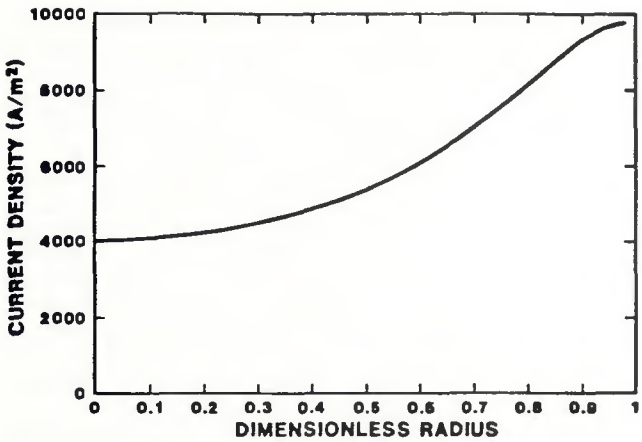

Fig. 3 — Calculated current density distribution on the workpiece

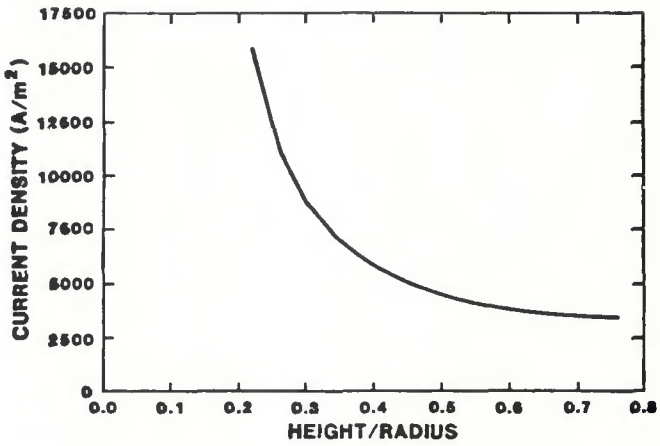

Fig. 4 — Calculated current density distribution on the probe

the ions. If it is assumed that electron interactions in the vapor are similar to those in air, k may be estimated for temperatures less than 10,000 K by (Ref. 9)

$$k = \frac{2m_e}{m_i} + 0.008\,\frac{3kT_e}{2e} \qquad (11)$$

The first term on the right side of Equation 11 is the mean fraction of energy lost per elastic collision, and the second term is a crude estimate of the energy fraction lost by inelastic collisions. If energy loss data are available for the vapor of interest, a more accurate estimate of k should be used.

T_e is obtained by iteratively solving Equations 10 and 11, and an expression for electron temperature Equation 12

$$T_e = \frac{m_e\, c_e^2}{3k} \qquad (12)$$

The field enhanced electron density, n, is then found by multiplying the equilibrium number density, n_o, by the Saha factor (Ref. 10) $\exp\left(\frac{\phi_i e}{kT_i}\left(1 - \frac{T_i}{Te}\right)\right)$.

If there is a significant change in conductivity due to field enhanced electron density, the electric potential ϕ in the core-flow region must be calculated from an equation derived from the continuity of current density, $\nabla \cdot \vec{j} = 0$, instead of the Laplace equation,

$$\nabla^2\phi = -\frac{\nabla\phi \cdot \nabla\sigma}{\sigma} \qquad (13)$$

where ϕ is the electric potential.

Experimental Procedure

The electrostatic probe tests were conducted with a pulsed Nd:YAG laser (1.06 μm wavelength). The welding parameters were as follows: 7.2-ms pulse duration, 10-Hz pulse frequency, and a laser energy of 14.2 J per pulse. The focal length from the lens to the workpiece was 114.3 mm (4.5 in.), and the laser spot diameter was 0.91 mm (0.035 in.) at the surface of the workpiece.

A schematic diagram of the electrostatic probe circuit is shown in Fig. 5. The electric probe, as shown in Fig. 1, consisted of a 0.254-mm (0.010-in.) thick sheet of molybdenum (25.4 mm wide and 76.2 mm long/1 × 3 in.), which was drilled with an array of 1-mm (0.04-in.) diameter holes. This arrangement allowed each test to be conducted on a new hole, which provided more consistent test results. The top surface of the molybdenum electrode was electrically insulated with a single layer of Kapton film 0.0635 mm thick (0.002 in.), and the bottom surface of the molybdenum was covered with two layers of Kapton film 0.127 mm (0.005 in.) thick. The drilled holes were covered with Kapton and punched to expose the inner cylindrical surface of the hole to the vapor plume. The surface of the workpiece was grit blasted with 50-μm-diameter alumina particles to provide a uniform surface roughness. The molybdenum electrode was then clamped securely on the top of the workpiece. Both the molybdenum electrode and the workpiece were attached to an x-y table. This allowed the laser to be easily repositioned to center of a hole.

Different power settings were provided by a power supply. The circuit current was determined by measuring the voltage drop across a 1-KΩ resistor ($V_{resis.}$). The voltage across the power supply was also measured ($V_{power\ supply}$) to insure that a constant voltage was maintained during the tests. The voltage drop across the probe was calculated by;

$$V_{electrode} = V_{power\ supply} - V_{resis.} \qquad (14)$$

A Nicolet 4094 oscilloscope was used to measure the two voltages and the laser pulse as a function of time. The voltage traces on the oscilloscope were set to trigger simultaneously with the laser pulse. After a particular test, a check was made to insure that the electric probe circuit was not shorted before another test was conducted. Tests results were obtained for power supply settings ranging from +10 V to −25 V. The negative power supply voltage implies that the hot electrode (workpiece) is now positive. This arrangement provides information on the saturation current. Results were also obtained for an open circuit whereby the power supply is removed and the 1-KΩ resistor is replaced by a 1-MΩ resistor.

Experimental Results

Figure 6 shows a typical voltage trace

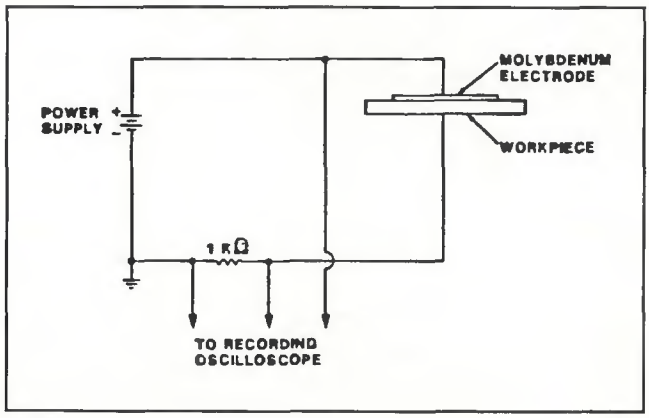

Fig. 5 — Circuit diagram for probe circuit measurements

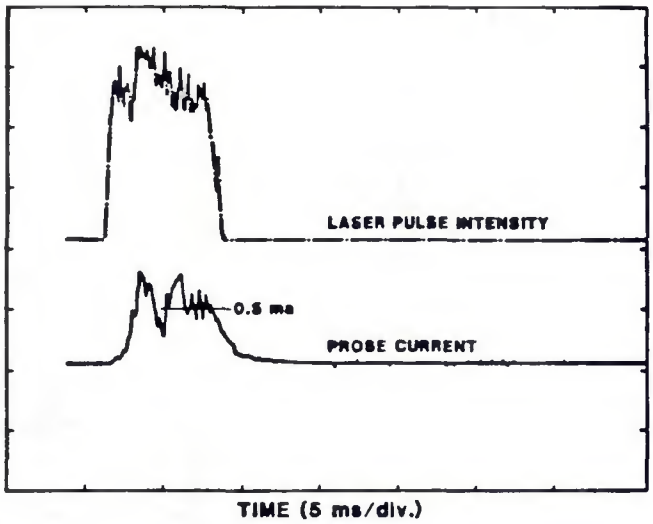

Fig. 6 — An oscillogram of probe current during a laser pulse

across a 1000-ohm resistor in series with the probe. This voltage is proportional to the probe current. As can be seen, the current varies with time as the vapor plume forms and decays. A visually averaged value near the peak current (horizontal line) is taken to represent the datum for this pulse. Open-circuit voltages across the probe (across a 1-megohm resistor) showed a time-varying signal in which the workpiece was initially positive (due to thermionic emission), then negative (indicating a higher temperature and floating potential of the vapor adjacent to the boiling surface over that of the probe surface), and then relaxing to zero near the end of the pulse (indicating equilibration of the temperature, probably due to condensation near the probe surface). When possible, data were taken from peaks near the end of the pulse.

The theoretical current-voltage characteristics at several temperatures for the cylindrical probe used are shown in Fig. 7, along with data taken from a series of experiments on Type 1100 aluminum. In calculating these curves, the electron collision frequency in aluminum vapor must be used. Apart from the alkali metals and mercury, there is not much data available for collision cross-sections of electrons in metal vapors. Estimates of the collision frequency were made as follows. The ion saturation current of the probe when the workpiece is positive (left edge of Fig. 7) is a function of number density and temperature, and is theoretically independent of collision frequency. If chemical equilibrium is assumed, the temperature is then determined. The right side of the characteristic is a function of number density, temperature and collision frequency. If the collision frequency is adjusted so that all the data cluster around the same temperature curve, an estimate of the collision cross-section can be made. This is consistent with the assumption of constant temperature in the plasma, which is not necessarily correct. The vaporization temperature of aluminum at one atmosphere is $\approx$2700 K. The data taken tend to cluster around 3000 K. The collision cross-section for electrons in aluminum vapor is then calculated to be 3.7×10^{-18} m^2, approximately equal to that for electrons in cesium vapor at the same energy (Ref. 11).

Almost all the data taken for aluminum fall in the temperature range of 2700 to 3300 K. Spectroscopic data taken by Peebles (Ref. 1) for similar energy pulses indicated temperatures that were slightly higher ($\approx$3500 K). The spectroscopic technique used however is most sensitive to the higher temperature portions of a gas with spatial temperature variations, whereas the probe technique is limited by the presence of low-temperature regions so this discrepancy is not surprising.

A similar procedure was carried out for experiments on mild carbon steel. The calculated current-voltage curves shown in Fig. 8 are for pure iron. Since the ionization potential and work function for carbon are higher than those of iron, it was considered that this was a suitable approximation. The vaporization temperature of iron is $\approx$ 3000 K, and again it is seen that the data cluster around a temperature that is higher than this value (3500 K). The electron collision cross-section for this case was found to be 2.2×10^{-18} m^2.

Conclusions

An electrostatic probe, and the theory for interpreting the data from it, have been developed for performing diagnostics on pulsed laser beam welding plumes. Data taken from aluminum and steel samples indicated plume temperatures that were only slightly higher than the vaporization temperatures, which agrees with spectroscopic measurements. No evidence of plasma breakdown or highly nonequilibrium electron densities were observed at the power densities used (3000 W/mm^2) in open atmosphere welds. More recent unpublished spectroscopic observations by H. C. Peebles indicate that in oxygen-free environments, high electron densities are

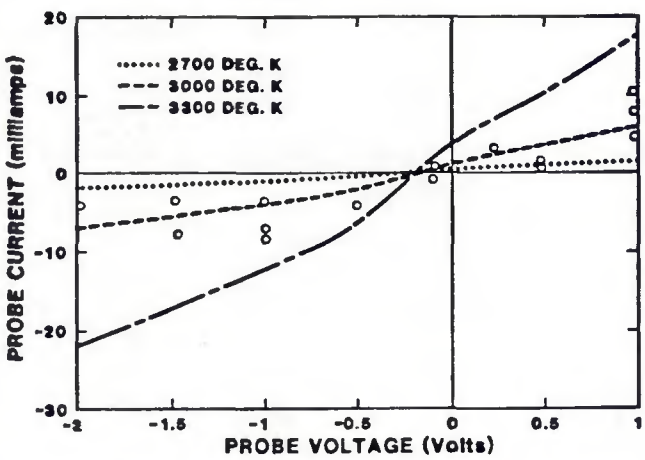

Fig. 7 — Probe current/voltage characteristics for aluminum 1100. Circles are measured data

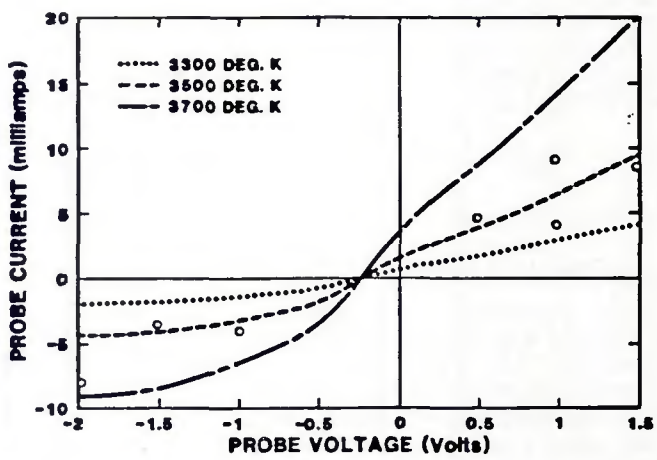

Fig. 8 — Probe current/voltage characteristics for iron. Circles are measured data

observed even at low powers. The use of probes to independently verify and investigate these results is therefore of importance to welding research and modeling efforts.

One of the disadvantages of using conductivity-sensitive probes is the requirement that the electron collision cross-sections with the various material vapors should be known for proper data interpretation. This difficulty was partially avoided in the present study by assuming constant temperature in the core-flow plasma and using the ion-saturation current to the cool electrode to estimate the collision cross-sections. The probe current is inversely proportional to the collision cross-section but varies exponentially with temperature so that an error in collision cross-section does not radically affect the temperature and number density estimates. The sparsity of data, however, must be seen as a limitation on the accuracy of probe techniques.

Open-circuit measurements of probe voltage indicate that the isothermal plasma assumption is only correct for part of the vapor plume duration. At early times, the plasma temperature over the workpiece seems to be higher than that of the plasma sweeping across the probe. During the last half (approximately) of the pulse, the open-circuit voltage goes to a small value indicating a small difference of temperature at the sheath edges.

Because of the low-temperature insulation used in the probe, it was not practical to reuse the same probe for successive measurements. Indeed, when used in that way, circuit shorts were more likely to develop. It is believed this can be alleviated by better probe construction.

References

1. Peebles, H. C., and Williamson, R. L. 1987. The role of the metal vapor plume in pulsed Nd:YAG laser welding on aluminum 1100. *Proc. Int. Conf. on Laser Advanced Material Processing,* Osaka, Japan, 1AO3.
2. Chung, P. M., Talbot, L., and Touryan, K. J. 1975. *Electric Probes in Stationary and Flowing Plasmas,* Springer-Verlag, N.Y.
3. Fedele, J. 1970. Survey of electrostatic probe theories. Aerospace Report No. TR-0059 (5681 6-42)-1.
4. Russo, A. J. 1972. A numerical solution of the two-dimensional flush mounted electrostatic probe problem. SC-RR-72 0111.
5. Gray, T. S. 1954. *Applied Electronics.* John Wiley, N.Y., pp. 77 and 131.
6. Kohl, W. H. 1960. *Materials and Techniques for Electron Tubes.* Reinhold Pub. Co., N.Y., p. 526.
7. Chang, K. W., and Bienkowski, G. 1970. Effects of electron emission on electrostatic probes at arbitary pressures. *Phys. Fluids* 13:902.
8. Von Engel, A. 1965. *Ionized Gases.* Oxford Univ. Press, London, England, pp. 126 and 123.
9. Reilly, J. P. 1965. Microwave breakdown of the air around a conical re-entry vehicle. *Avco Everett Research Report 214.*
10. Mitchner, M., and Kruger, C. H. 1973. *Partially Ionized Gases.* John Wiley & Sons, N.Y., p. 231.
11. Gilardini, A. 1972. *Low Energy Electron Collisions in Gases.* John Wiley & Sons, N.Y., p. 421.